

# Interfacial Microstructure, Microhardness and Tensile Properties of Al Micro-Particle Doped Sn-9Zn Eutectic Pb-Free Solder Alloy for Microelectronics Applications

Sheik Md. Kazi Nazrul Islam<sup>1,2</sup>, Ahmed Sharif<sup>2,3</sup>, T. Alam<sup>2</sup>

<sup>1</sup>University of Information Technology and Sciences (UITS), Dhaka, Bangladesh

<sup>2</sup>Bangladesh University of Engineering and Technology, Dhaka, Bangladesh

<sup>3</sup>Nanyang Technological University, Singapore 639798

*s.m.k.nazrulislam@gmail.com*

**Abstract**— In this study, the effect of Al micro-particles (10 $\mu$ m) to Sn-9Zn eutectic solder, were examined in order to investigate the microstructural and mechanical properties as well as thermal behavior of the newly developed ternary solder alloys. Here, an approach to prepare a micro-composite solder alloy by mixing Al with a molten Sn-Zn solder alloy was developed. The composite solder was prepared by mechanically mixing Al micro-particles into the Sn-9Zn alloy melt to ensure a homogeneous distribution of the reinforcing particles. The Al particles reacted with the Zn and formed intermetallic compounds (IMC) with the eutectic solder alloy. The microstructures of newly developed ternary Sn-9Zn-xAl solder alloys contain fine needle-like  $\alpha$ -Zn phase with some IMCs dispersed in the  $\beta$ -Sn matrix. The compact shaped Al<sub>3</sub>Zn<sub>3</sub>Sn IMC uniformly distributed in the  $\beta$ -Sn phase which results in an increase in the tensile strength, due to the second phase dispersed strengthening mechanism. As the Al content increases, the microhardness of the Sn-9Zn-xAl ternary solder alloys also improves due to the presence of harder IMC in the microstructure. The thermal behavior was found in the sustainable working range for these composite solders.

**Index Terms**— Al micro-particles, lead-free solder, tensile properties, intermetallic compounds.

## I. INTRODUCTION

The importance of reflow soldering in electronic packaging is increasing due to the rapid growth of the electronic industry in recent years. Traditionally, Sn-Pb solders were extensively used for interconnections in electronic components due to their unique combination of mechanical properties, superior wetting properties, moderate melting temperatures and low cost [1–3]. Environmental and health concerns over the toxicity of lead combined with strict legislation to ban the use of lead-based solders have provided an inevitable driving force for the development of lead-free solder alloys [4,5]. Therefore, establishing a lead-free solder has become a critical issue. In fact many research groups have been focused on developing new solders. But new solders must fulfill several requirements such as wettability, a suitable melting temperature, good mechanical properties, good resistance to mechanical and thermal fatigue, corrosion resistance, good electrical properties, good for health and the environment, availability and low material cost [6,7]. Recently, several types of new Pb-free Sn-base solders such as Sn-Zn, Sn-Ag and Sn-Ag-Cu have attracted the attention of the electronics

industry [8]. Among them the eutectic or near eutectic Sn-Zn solders have been recognized as candidates for Pb free solder materials due to their low cost and low melting points. The melting point of the eutectic Sn-9Zn wt.% solder is 198 $^{\circ}$ C which is close to that of the conventional Sn-Pb (183 $^{\circ}$ C) eutectic alloy and is much lower than that of other Sn-based alloys e.g. Sn-Cu (227 $^{\circ}$ C), Sn-Ag (221 $^{\circ}$ C) and Sn-Ag-Cu (217 $^{\circ}$ C) [9,10].

In general, the reliability of a solder joint plays an important role in determining the lifetime of electronic devices. This reliability is mainly dependent on matching the coefficient of thermal expansion, having a high elastic modulus, hardness, yield strength and shear strength together with resistance to corrosion, fatigue and creep [11]. Studies have shown that a potentially viable and economically affordable approach to improve the mechanical properties of a solder is to add an appropriate second phase particles, of ceramic, metallic or intermetallic, to a solder matrix so as to form a composite. The formation, presence and growth of the second phase have been proposed as a potential mechanism that controls solderability [12]. Lin et al. studied the influence of reinforcing TiO<sub>2</sub> and Cu particles on microstructural development and hardness of eutectic Sn-Pb solders, and the measured microhardness revealed that the addition of TiO<sub>2</sub> and Cu particles enhanced the overall strength of the eutectic solder [13]. Mavoori and Jin [14] used TiO<sub>2</sub> and Al<sub>2</sub>O<sub>3</sub> particles as the reinforcement for a conventional 63Sn-37Pb solder and reported a significant enhancement in creep resistance and also in other mechanical properties. Mohan et al. prepared Sn-Pb composite solders by the addition of single wall carbon nano-tubes (SWCNT) as the reinforcing agent and reported that the mechanical properties of these composites such as hardness, yield strength and ultimate tensile strength were found to be superior to the unreinforced solder, while the melting point was not appreciably altered [15]. The Al may form solid solutions with Zn and Sn and has a eutectic point at 197 $^{\circ}$ C as reported by Sebaoun et al., who discussed the diffusion paths of various Sn-Zn-Al systems at various isotherms [16]. It has been reported that the Al-Zn-Sn solders have good wettability on Al [17]. The microstructures of the Sn-9Zn-0.45Al lead-free solders have been investigated using scanning electron microscopy [18].

In the present study, addition of a third element

significantly changes Sn-9Zn eutectic binary alloys microstructure, and mechanical properties. It has already proven that addition of a third element in the Sn-9Zn eutectic solder greatly improves its mechanical properties [19-21]. Thus, the objective of this study is to find out the relation between the microstructure and mechanical properties that alters with the formation of IMCs for various amount of Al addition. This study concerns with the melting temperature, microstructure, microhardness and tensile properties on Sn-9Zn eutectic solder alloy that may alter after addition of various amount of Al in it.

The remainder of the article is organised as follows. The next section briefly describes about experimental procedure of lead-free composites solder. The third section would present the discussion regarding the results of the newly developed ternary solder alloys. Finally we abrogate the article with a short concluding remarks and acknowledgement of the research work.

## II. EXPERIMENTAL PROCEDURE

The Sn-9Zn, Sn-9Zn-1.0Al, Sn-9Zn-2.0Al and Sn-9Zn-4.0Al lead-free solders were prepared with commercially available pure tin, zinc, and copper (purity of 99 %). The constituent elements were melted in the alumina crucible inside a furnace. The molten alloys were homogenized at 300°C and then poured in a steel mold to prepare the chill cast ingot. Consequently, chemical analyses were done by volumetric method to determine the exact composition of the casting ingots. The chemical compositions of the alloys are listed in Table 1. The melting temperatures of the solder alloys were determined with differential scanning calorimeter (DSC Q 10). For DSC analysis, 10 mg solder was placed into an Al pan. To obtain the data, the sample was initially scanned from 25°C to 150°C at a rate of 25 K min<sup>-1</sup> and then at a rate of 5 K min<sup>-1</sup> up to 250°C under nitrogen gas atmosphere.

The as-cast solders were sectioned and polished according to non-ferrous metallography with 0.5µm Al<sub>2</sub>O<sub>3</sub> particles in order to obtain the microstructure. After cleaning with acetone and alcohol, the samples were investigated by an optical microscope with digital camera (LEICA-MZFLIII), and as well as with SEM. A Philips XL40 FEG scanning electron microscope (SEM) equipped with an energy dispersive X-ray (EDX) analysis system was used to inspect and analyze the microstructure of the three different solders and to perform the semi quantitative analysis on those structures in order to determine the phases. The accuracy of the compositional measurement was about 5%. To determine the formula composition of the intermetallic compounds (IMCs), the chemical analyses of the EDX spectra were corrected by standard ZAF software. The backscattered electron imaging mode of the SEM was used for the microstructural study. EDX analysis has been done to support the phase identification of the structure. Grinding and polishing were necessary to obtain polished, smooth and flat parallel surface before indentation testing. Thus, the polished samples were placed in a Brinell hardness tester to measure the microhardness. The applied

load was 1.2 kN for thirty seconds and at least ten readings of different indentation were taken for each sample at room temperature to obtain the mean value.

Table 1  
Chemical composition of starting materials (wt. %)

Alloys	Sn	Zn	Al	Pb	Bi	Sb
Sn-9Zn	Bal.	8.69	-	0.35	0.23	0.01
Sn-9Zn-1.0Al	Bal.	8.68	0.98	0.34	0.25	0.02
Sn-9Zn-2.0Al	Bal.	8.60	2.01	0.35	0.25	0.01
Sn-9Zn-4.0Al	Bal.	8.63	3.96	0.34	0.26	0.01

The tensile specimens with a gauge length marked 32.00 mm were prepared by machining and the other dimensions are mentioned in figure 1. The width and thickness of the samples were 6.00 mm and 5.00 mm respectively. Tensile tests were carried out with a tensile testing machine (Instron 3369 Universal Testing Machine) at a strain rate of 1.00 mm/min at 25°C to obtain data on the stress-strain curves which contain information of elongation at fracture and the UTS.

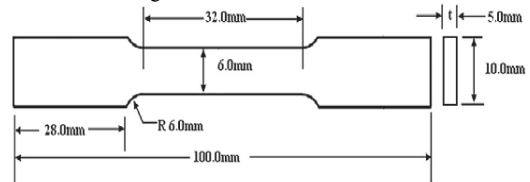


Figure 1: Schematic diagram of the tensile specimen.

## III. RESULTS AND DISCUSSIONS

DSC analysis was carried out in order to investigate the fundamental thermal reactions on heating of these alloys. Figure 2 shows the typical DSC curves obtained for Sn-9Zn, Sn-9Zn-1.0Al, Sn-9Zn-2.0Al, and Sn-9Zn-4.0Al alloys on heating. With the addition of small amount of Al, the melting temperatures changed slightly. The melting temperatures were found 201.71°C, 203.15°C and 205.40°C for the Sn-9Zn-1.0Al, Sn-9Zn-2.0Al, and Sn-9Zn-4.0Al, respectively, as compared with 197.59°C for Sn-9Zn eutectic alloy. It was reported earlier that the addition of a small amount of Al did not significantly alter the melting point of the Sn-9Zn alloy [22]. Here, for 4% Al addition the melting temperature increases about 8°C than that of Sn-9Zn binary eutectic alloy.

Table 2  
Melting temperature and mechanical properties  
of Sn-9Zn, Sn-9Zn-1.0Al, Sn-9Zn-2.0Al, and Sn-9Zn-4.0Al alloys

Alloys	Melting Temp. (°C)	Micro-hardness (BHN)	Ultimate Tensile Strength (MPa)	Elongation (%)
Sn-9Zn	197.59	16.80	41	48.00
Sn-9Zn-1.0Al	201.71	18.10	51.24	24.53
Sn-9Zn-2.0Al	203.13	19.15	52.57	32.67
Sn-9Zn-4.0Al	205.40	20.15	55.55	27.06

The optical and SEM micrograph of the Sn-9Zn in Figure 3 (a and b) shows the typical lamella of eutectic microstructure. It has been mentioned that the eutectic Sn-9Zn alloy consists of  $\beta$ -Sn and Zn-rich phases. In the micrograph, the bright regions are the  $\beta$ -Sn phase and the primarily solidified phases; the dark phases are fine needlelike Zn-rich phase in  $\beta$ -Sn matrix. Also some Zinc spheroids are observed in the microstructure.

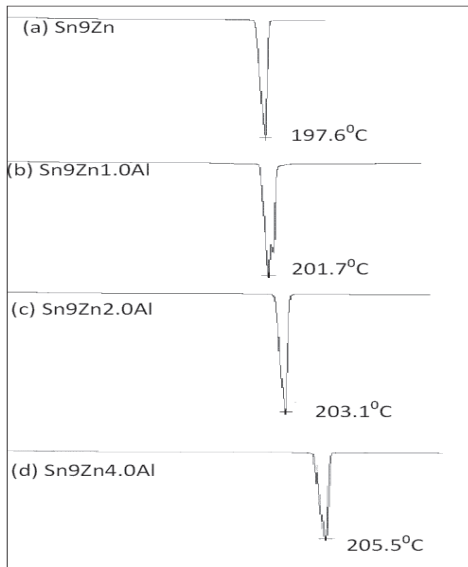


Figure 2: DSC curves of Sn-Zn-Al micro-composite solder alloys on heating

With the addition of 1% Al, the eutectic Sn-9Zn alloy shows some precipitates distributed in the eutectic phase shown in Fig. 3 (c and d). When 2% Al is added with the eutectic Sn-9Zn alloy, the microstructure changes with globular shaped intermetallic compound distributed in the typical eutectic lamella as shown in Figure 4 (a and b). After the Al addition increases to 4% the number of intermetallics also increases while eutectic phase decreases and at the same time IMC size become little larger, as shown in Figure 4 (c and d). The micrograph of the ternary alloys can be distinguished into three phases, i.e. the matrix  $\beta$ -Sn, the needle-like eutectic  $\alpha$ -Zn, and the globular dark grey phases. EDX analyses were carried out to clarify the composition of the dark grey phases. As can be seen in Figure 5 (a and b), the dark grey phases revealed that the phases are composed of Al, Sn and Zn and the Al percentage of these phases are about 57 at. %. This observation implies that these dark grey phases are actually  $Al_6Zn_3Sn$  IMC.

Thus, we can see when a third element Al is added with the Sn-9Zn eutectic alloy, the  $\alpha$ -Zn phases decreases and changes to finer structure. As Zn is a very reactive material (electro negativity: -1.65), it forms compound readily with the Al. With these reactions, the microstructure of Sn-9Zn-2.0Al and

Sn-9Zn-4.0Al deprives of thick Zn-rich eutectic lamella and consists of fine eutectic colonies dispersed with large  $Al_6Zn_3Sn$  compounds.

The microhardness of a solder alloy depends on the motion of dislocation, growth and configuration of grains. The processes are more sensitive to the microstructure of the solder alloy than its chemical composition. So the mechanical property such as the microhardness depends especially on the microstructure, processing temperature, the composition, etc. [23]. In the present study the microhardness test was performed to observe the change of mechanical properties associated with the microstructural changes. Figure 6 shows the microhardness results with standard deviation as a function of alloy composition. In general, the hardness of Sn-based solders strongly depends on the alloying elements; the more the alloying elements, the higher the hardness. This is attributed to the fact that the volume fraction of the other phases increases as there are more alloying elements in solder. The same trend was confirmed for Sn-9Zn-xAl alloys; the average hardness value increases when Al is added to the Sn-9Zn eutectic alloy as a third alloying element, as shown in Figure 6.

As summarized in Table 2 the BHN of eutectic Sn-9Zn was 16.8, while those of Sn-9Zn-1.0Al, Sn-9Zn-2.0Al, and Sn-9Zn-4.0Al were 17.89, 19.15 and 20.15 respectively. The hardness increases for Sn-9Zn eutectic alloy after addition of a third element can be understood by dissolution of Al atoms for Sn-9Zn-xAl ternary alloys and formation of IMC particles in the solder matrix to promote precipitation hardening. This may also be explained by the microstructural observations for the corresponding ternary alloy. Figure 4 represents that all the Sn-9Zn-xAl alloys are composed of three different phases; the matrix  $\beta$ -Sn, small amount of needle-like eutectic  $\alpha$ -Zn, and the dark gray phases of IMCs, while the Sn-9Zn eutectic alloy consists of only first two phases with some Zn spheroids in it.

The effect of third alloying additives on mechanical properties of Sn-9Zn eutectic solder alloy can also be seen from the strain-stress curves shown in Figure 7. The ultimate tensile strength (UTS) and elongation values are listed in Table 2. The tensile strength of the Sn-9Zn, 9Zn-1.0Al, Sn-9Zn-2.0Al, and Sn-9Zn-4.0Al were 48.78, 51.24, 52.57 and 55.55 MPa, respectively. The elongation at failure of the Sn-9Zn, 9Zn-1.0Al, Sn-9Zn-2.0Al, and Sn-9Zn-4.0Al were 48, 24.5, 32.6 and 27%, respectively. The Sn-9Zn-4.0Al alloy shows the highest UTS, while Sn-9Zn alloy exhibits the highest elongation and the lowest UTS. As per dispersion strengthening theory [24], the strength must increase with the addition of a second phase particle in the matrix. The both phenomenon of tensile strength and elongation can be clearly explained by the dispersion strengthening theory; i.e. the second phase formed by Al generates obstacle for the dislocation at the grain boundary (the maximum region of mismatch), dislocation piles up results in a increase in tensile strength, the term also called precipitation strengthening. On the other hand due to movement restriction of dislocation densities the slip planes cannot find their suitable direction to move freely results lack in ductility; i.e. elongation decreases.



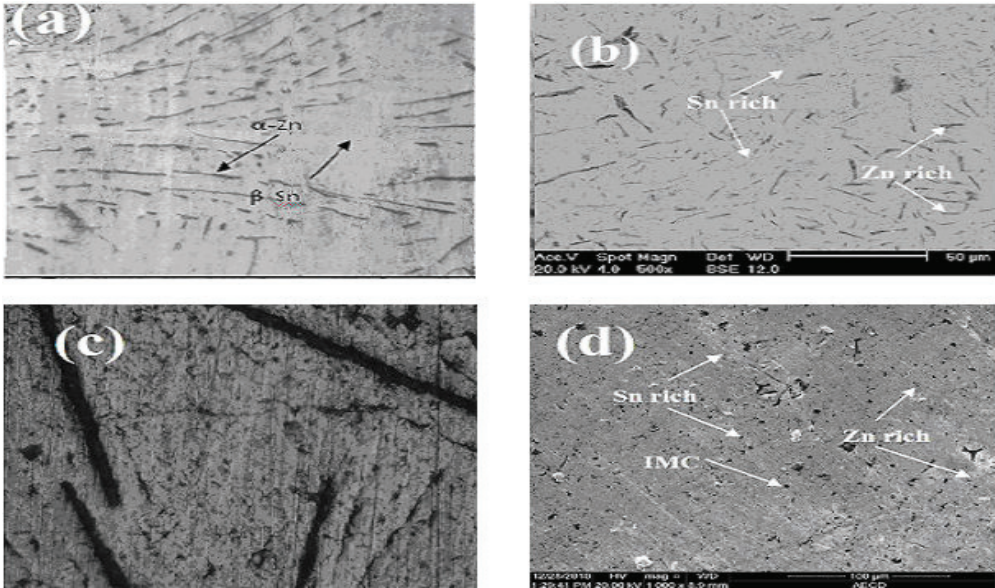


Figure 3: (a) Optical micrograph of Sn-9Zn (b) SEM micrograph of Sn-9Zn (c) Optical micrograph of Sn-9Zn-1.0Al (d) SEM micrograph of Sn-9Zn-1.0Al

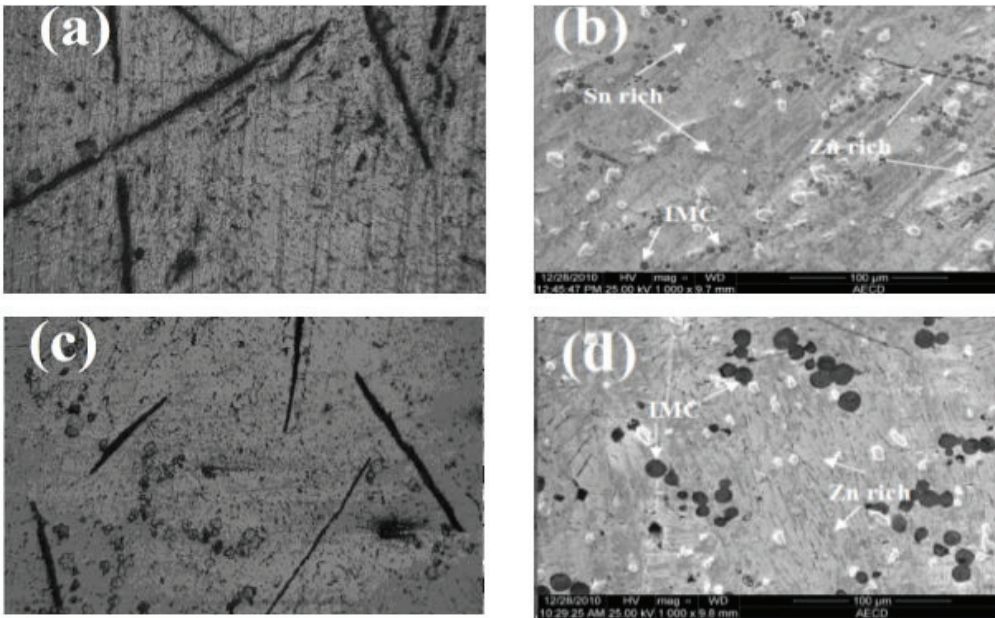


Figure 4: (a) Optical micrograph of Sn-9Zn-2.0Al (b) SEM micrograph of Sn-9Zn-2.0Al (c) Optical micrograph of Sn-9Zn-4.0Al (d) SEM micrograph of Sn-9Zn-4.0Al

REFERENCES

- [1] M. Abteew, G. Selvaduray, *Mater. Sci. Eng. R* 27 (2000) 95–145.
- [2] A. Sharif, Y.C. Chan, *J. Alloys Compd.* 393 (2005) 135–140.
- [3] K.K. Mohan, V. Kripesh, L. Shen, K. Zeng, A. A. O. Tay, *Mater. Sci. Eng. A* 423 (2006) 57–63.
- [4] A. Sharif, Y.C. Chan, *Mater. Sci. Eng. A* 445-446 (2007) 686–690.
- [5] A. Sharif, Y.C. Chan, *J. Alloys Compd.* 440 (2007) 117–121.
- [6] J. Wan, Y. Liu, C. Wei, Z. Gao, *J. Alloys Compd.* 463 (20 08) 230–237.
- [7] T.C. Chang, Y. T. Hsu, M.H. Hon, M.C. Wang, *J. Alloys Compd.* 360 (20 03) 217–224.
- [8] M.N. Islam, Y.C. Chan, A. Sharif, M.J. Rizvi, *J. Alloys Compd.* 396 (2005) 217–223.
- [9] S. Vaynman, M.E. Fine, *Scripta Mater.* 41 (12) (1999) 1269–1271.
- [10] T. Ichitsubo, E. Matsubara, K. Fujiwara, M. Yamaguchi, H. Irie, S. Ku mamoto, T. Anada, *J. Alloys Compd.* 392 (20 05) 20 0–205.
- [11] Date M, Shoji T, Fujiyoshi M, Sato K, Tu KN. Ductile-to-brittle transition in Sn–Zn solder joints measured by impact test. *Ser Mater* 2004;51:641–5.
- [12] Guo F, Lee J, Choi S, Lucas JP, Bieler TR, Subramanian KN, et al. Sn–3.5Ag solder reinforced with mechanically incorporated Ni particles. *J Electron Mater* 2001;30:1073–82.
- [13] Lin DC, Wang GX, Srivatsan TS, Al-Hajri M, Petraroli M. Influence of titanium dioxide nanopowder addition on microstructural development, hardness of tin–lead solder. *Mater Lett* 2003;57:3193–8.
- [14] Mavoori H, Jin S. New, creep-resistant, low melting points with ultrafine oxide dispersions. *J Electron Mater* 1998;27:1216–22.
- [15] Mohan KK, Kripesh V, Tay AAO. Influence of single-wall carbon nanotube addition on the microstructural, tensile properties of Sn–Pb solder alloy. *J Alloys Compd* 2008; 455:148–58.
- [16] A. Sebaoun, D. Vincent, D. Treheux, “Al-Zn-Sn phase diagram isothermal diffusion in ternary system” *Mater. Sci. Technol.* 3 (1987) 241-248.
- [17] K. Sugauma, T. Murata, H. Noguchi, Y. Toyoda, “Heat resistance of Sn–9Zn solder/Cu interface with or without coating” *J. Mater. Res.* 15 (2000) 884-891.
- [18] S. P. Yu, M. C. Wang, M.H. Hon, “Formation of Intermetallic compounds in Eutectic Sn-Zn-Al-solder hot-dipped on Cu substrate” *J. Mater. Res.* 16 (2001) 76-82.
- [19] D. Soares, C. Vilarinho, J. Barbosa, R. Silva, M. Pinho and F. Castro, “Effect of the Bi content on the mechanical properties of a Sn-Zn-Al-Bi solder alloy”, *Mater. Sci. Forum* 455- 456 (2004) 307-311.
- [20] C. M. Chuang, T. S. Lui, L. H. Chen, “Effect of aluminum addition on tensile properties of naturally aged Sn-9Zn eutectic solder”, *J. Mater. Sci.* 37 (2002) 191-195.
- [21] C. M. L. Wu, and Y. W. Wong, “Rare-earth additions to lead-free electronic solders”, *J. Mater. Sci.: Mater. Electron.* 18 (2007) 77-91.
- [22] S. K. Das, A. Sharif, Y. C. Chan, N. B. Wong and W. K. C. Yung, Influence of small amount of Al and Cu on the microstructure, microhardness and tensile properties of Sn-9Zn binary eutectic solder alloy, *J. Alloys and Compounds*, 481 (2009) 167-172.
- [23] D. Frear, H. Morgan, S. Burchett, J. Lau, “The Mechanics of Solder Alloy Interconnects”, Van Nostrand Reinhold, New York (1994).
- [24] G. E. Dieter, “Mechanical Metallurgy”, McGraw-Hill Book Co., New York (1986).

